Macromolecules

ARTICLE

pubs.acs.org/Macromolecules

Water−Polymer Interaction during Water Uptake

Viktor Baukh,[†] Hendrik P. Huinink,[*,†] Olaf C. G. Adan,[†,‡] Sebastiaan J. F. Erich,[†,‡] and Leendert G. J. van der Ven[§]

[†]Department of Applied Physics, Eindhoven University of Technology, P.O. Box 513, NL-5600MB, Eindhoven, The Netherlands

[‡]TNO, Delft, The Netherlands

[§]AkzoNobel Automotive & Aerospace Coatings, Sassenheim, The Netherlands

ABSTRACT: Water uptake by multilayer films plays an important role in their performance. Individual layers may consist of different polymeric phases. Understanding the water uptake in such systems requires knowledge of the water distribution, its state in the polymer, and influence on the polymeric phases. This study illustrates the application of high-resolution NMR and relaxometry for measuring water distributions and evaluating water−polymer interactions. We studied water uptake in a two-layered base coat/top coat system, where the base coat consisted of acrylic, polyurethane, pigment particles, and a polymeric dispersant. Water and the polymer phases in the base coat were identified with NMR relaxometry. The water diffusivity in the base coat was determined. At high water contents water is highly mobile and is loosely bonded to the polymer. Reversible plasticization of the dispersant was observed. The polymeric dispersant seems to play a key role in the sorption of water by the coating.

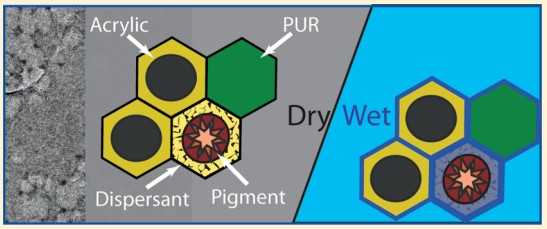

INTRODUCTION

Organic coatings play an important role in protection and aesthetic appearance of various substrates. Mostly, these coatings consist of several layers to meet industrial or end-user specifications. The top coat layer normally plays the role of a barrier, protecting the substrate from weathering and giving a glossy appearance, whereas underlying layers, such as a base coat layer and primer, define the color and introduce functions like adhesion and corrosion protection, respectively.[1] Furthermore, many of these layers are heterogeneous in nature, as they consist of different polymeric and inorganic phases.

The penetration of water into organic coatings plays an important role in the performance of the coating and deterioration of the coated substrate, justifying a profound study of water transport processes in organic coatings. Various techniques are used to probe water uptake by coatings and polymeric films, such as gravimetry, electrochemical impedance spectroscopy,[2−4] Fourier transform infrared spectroscopy (FTIR),[5−7] and fluorescent spectroscopy.[8] From the listed techniques only FTIR is able to probe distribution of water in the direction parallel to the coating/substrate interface.[6,7] It is also known that FTIR provides information about the interaction between polymer and water.[9] In the case of multilayered films an adequate interpretation of water absorption requires information about the water distribution as a function of the position perpendicular to the surface. Thus, the inability to probe such water distribution is a major drawback of the mentioned techniques. Except for FTIR, none of these techniques are able to probe specific interactions between water and the different polymeric phases within a layer.

The major part of the published literature concerns water in single layer organic coatings and polymeric films.[10] Only a few studies are dedicated to water uptake in multilayer films.[2,4,11,12] Carbonini et al.[11] studied the effects of the chemical composition of the constituent layers on the water uptake in a multilayer system. They showed that water absorption and degradation of the multilayered systems depend on the chemical characteristics of each layer and on the layer position in the system.[2] Allahar et al.[4] pointed out that the layer interface can play an important role in transport of water in multilayer coatings. Recently, we have studied water uptake in multilayer coatings with high-resolution NMR imaging. The ingress of water into a waterborne base coat through a protective top coat was visualized.[12] Water distributions and swelling were measured simultaneously as a function of time, and the barrier properties of the top coat were estimated. A thermodynamical model was formulated to describe the process. Profound knowledge of the state of water in the polymer matrix is needed to make a next step toward a full understanding of the process. Therefore, the influence of penetrated water on the polymeric material in the multilayered film should be studied.

In principle, NMR has also the potential to probe the interaction of water with the different polymer phases within a layer. Besides its ability to image, an additional feature of NMR is its ability to obtain information about diffusivity of liquids[13] and mobility of the polymer molecules.[14] The signal relaxation can be different for water and polymers. In the case of a polymer the relaxation time strongly depends on the mobility of polymer chains, being short for chains with low mobilities and long for highly mobilized chains. Consequently, plasticizing effects can be

Received: December 18, 2010
Revised: May 11, 2011
Published: May 18, 2011

determined, as it leads to increased mobility of the polymer chains.[15] Thus, combining high-resolution NMR imaging with NMR relaxometry seems to be a versatile technique for clarifying water uptake processes in thin multilayer polymeric films.

This paper presents a study using the potential of NMR to study the interplay between water and a polymer matrix during water uptake in a multilayer system. The considered polymer system is a two-layered base coat/top coat system, of which the top coat is a solventborne highly cross-linked system and the base coat is a physically dried waterborne system consisting of pigment particles, acrylic and polyurethane (PUR) particles. To disperse the pigment, a significant fraction of a polymeric dispersant is present in the base coat. This study addresses the interactions of water with the base coat, i.e., the state of water in the polymer matrix and its influence on the polymeric material. Water and base coat ingredients were identified with NMR relaxometry showing a rather high mobility of water in the wet base coat. The self-diffusion coefficient of water in the wet base coat was estimated, and the concentration dependency of the water mobility in the base coat was investigated. We observed reversible plasticization of the dispersant by water. The paper concludes with a discussion of the plasticizing mechanisms and the time dependency of the process.

THEORETICAL AND EXPERIMENTAL DETAILS

NMR Principles. *NMR Signal.* For imaging with NMR, the resonance frequency f and, thus, the magnitude of the magnetic field $|\vec{B}|$ should be position dependent. In the GARField approach proposed by Glover et al.[16] a magnetic field with a high static gradient is generated, enabling imaging with a high resolution of 3−6 μm.[12] In the region of interest the magnetic field is linear with the position $|\vec{B}| = B_0 + Gx$, where $G = \partial|B|/\partial x$ [T/m] denotes the gradient of the absolute value of the magnetic field and x is the direction perpendicular to the coating layer.[12,16]

To obtain the signal, various pulse sequences can be used.[17] A train of so-called spin echoes is obtained. In the case of N distinct ^{1}H pools the signal of the nth spin echo reads

$$S_n(x,t) = P_n(x)\sum_{k=1}^{N}\rho_k(x)[1-\exp(-t_r/T_{1k}(x))]\exp(-nt_e/T_{2k}(x)) \quad (1)$$

where k refers to a number of a specific ^{1}H pool and ρ_k [mol/m^3] is the density of ^{1}H nuclei of the kth specific pool. The pool k has longitudinal relaxation time T_{1k} [s] and transversal relaxation time T_{2k} [s]. Note that the mentioned parameters reflect properties of a sample. In contrast, the repetition time t_r [s] and interecho (interpulse) time t_e [s] are settings in the measurements. The function $P_n(x)$ is a weighing factor for the nth echo. It combines effects of the excitation and coil sensitivity profiles and evolution of coherent pathways in the used pulse sequences[18] and does not contain information about the measured sample.

Note that equally spaced pulses are assumed in eq 1. In the case that $t_r/T_{1k} \gg 1$ for all k, the T_1 factors in eq 1 are close to 1 and can be neglected. Thus, only T_2 weighing is left for each pool of ^{1}H nuclei.

$$S_n(x,f) = P_n(x)\sum_{k=1}^{N}\rho_k(x)\exp(-nt_e/T_{2k}(x)) \quad (2)$$

Relaxation Behavior. The T_2 time of the relaxation process characterizes the mobility[14,19,20] and diffusivity[13,18] of the measured species.

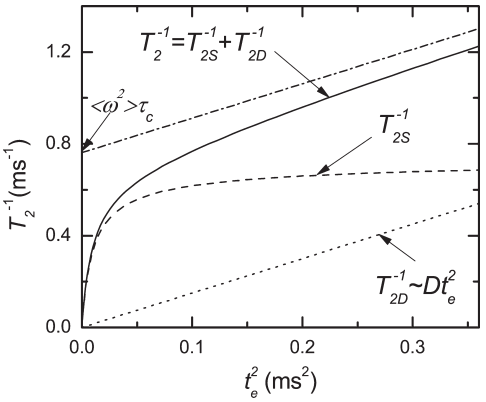

Figure 1. Typical behavior of the T_2 relaxation time as a function of t_e^2 for a system, completely dominated by diffusion in the field gradient (dotted line), dipolar interactions of the nuclei (no diffusion, dashed line). The solid line refers to the relaxation behavior governed by both dipolar interactions and diffusion. The dashed-dotted line shows the behavior when $\tau_c \ll t_e$.

If both diffusion and molecular mobility contribute to the relaxation process, the measured T_2 time will read

$$T_2^{-1} = T_{2D}^{-1} + T_{2S}^{-1} \quad (3)$$

where T_{2D} [s] is relaxation due to diffusion and T_{2S} [s] describes relaxation associated with the mobility of the measured species.

The relaxation due to diffusion in the field gradient is given by the following equation

$$T_{2D}^{-1} = \alpha\gamma^2G^2Dt_e^2 \quad (4)$$

where D [m^2/s] is a self-diffusion coefficient of the measured nuclei and t_e [s] is an echo time. The parameter α is a constant, which is defined by the evolution of coherent pathways for a given pulse sequence. For the detailed discussion of eq 4 we refer to Appendix A.

In our experiments an Ostroff−Waugh-like pulse sequence[21,22] is used. For this pulse sequence the relaxation time determined by the mobility of the measured species relates to the correlation time τ_c associated with molecular motions as follows[19,23]

$$T_{2S}^{-1} = \langle\omega^2\rangle\tau_c\left[1-\frac{\tanh(t_e/\tau_c)}{t_e/\tau_c}\right] \quad (5)$$

where $\langle\omega^2\rangle$ is the second moment associated with residual interactions.[24]

In the case $t_e/\tau_c \gg 1$ eq 3 reduces to $T_2^{-1} = \langle\omega^2\rangle\tau_c + \alpha\gamma^2G^2Dt_e^2$. In this regime all echo time dependency of T_2^{-1} is due to diffusion.

The dependency of T_2 on the echo time is shown in Figure 1 for τ_c = 60 μs, $\langle\omega^2\rangle$ = 12.7 ms^{-2}, and $\alpha\gamma^2G^2D$ = 1.5 ms^{-3}. The dotted line shows the relaxation time T_{2D} purely determined by diffusion, whereas the dashed line shows the behavior of the T_{2S}. The dashed-dot line shows the total T_2 time when T_{2S} equals the plateau $\langle\omega^2\rangle\tau_c$, whereas total T_2 is shown by the solid line. Given that $t_e/\tau_c \gg 1$, the slope of the curve is proportional to the self-diffusion coefficient of the measured species. The switch to the linear mode as well as the value of the plateau $\langle\omega^2\rangle\tau_c$ characterizes the mobility of the nuclei. Higher plateau values and later transition times indicate a lower mobility of the nuclei, showing that they are more tightly bonded. Lower plateau values and earlier transition indicates weaker binding of the measured nuclei.

dx.doi.org/10.1021/ma102889u |Macromolecules 2011, 44, 4863–4871

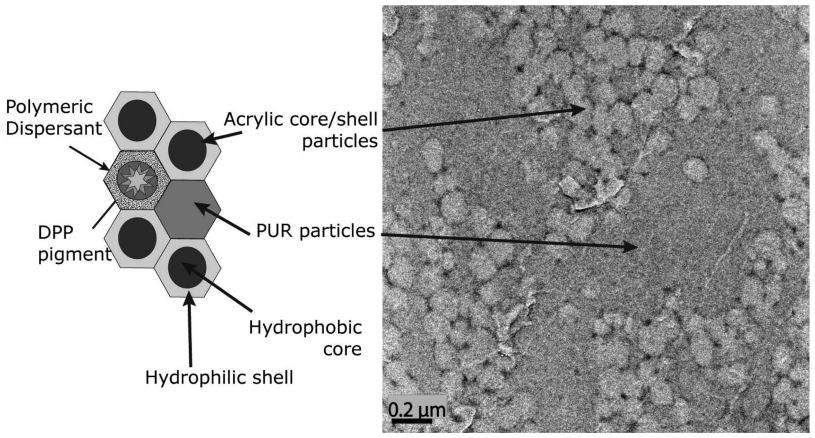

Figure 2. Schematic presentation of the polymer matrix of the base coat and TEM image of an unpigmented base coat (acrylic and PUR particles only).

Samples. The investigated polymeric systems are two-layered base coat/top coat (BC/TC) systems. The base coat consists of 40% w/w acrylic particles, 20% w/w polyurethane (PUR) particles, 30% w/w DPP (diketopyrrolopyrrole) pigment particles, and 10% w/w polymeric dispersant in the sample (see Figure 2).

The ingredients of the base coat material are as follows.[25] The acrylic particles are synthesized by emulsion polymerization and have a core/shell structure. The core consists of BA (butyl acrylate), BMA (butyl methacrylate), and HEMA (hydroxyethyl methacrylate). The shell is made from BA, MMA (methyl methacrylate), and MAA (methacrylic acid) and neutralized with DMEA (dimethylethanolamine). The shell/core volume ratio equals approximately 1:7, and their glass transition temperature T_g is about 25 °C. The PUR particles consist of hydroxyl functional carbonate and DMPA (2,2′-bis(hydroxymethyl)propionic acid) chain extended with isocyanate and neutralized with DMEA.[26] The T_g of the PUR particles is approximately equal to 0 °C. The polymeric dispersant is nonionic comb polymer with a backbone of styrene and maleic anhydride of and hydrophilic hairs of PEO (poly(ethylene oxide)) and PPO (poly(propylene oxide)). The total hydroxyl, acid, and amine numbers for the base coat are respectively 0.15, 0.25, and 0.15 mequiv/g base coat. As a consequence, these exchangeable protons will not influence the NMR signal height but still could influence the T_2 relaxation.

The morphology of the base coat film without pigment particles is investigated by TEM after cryosectioning and staining with Ba hydroxide (see Figure 2). Acrylic and PUR particles appeared to be clustered in aggregates of ∼1 μm. The PUR particles are not noticed as individual particles as seen for the acrylic particles. Either the boundaries between the PUR particles are not observed by TEM or the particles are interdiffused to a large extent.

The top coat is a two-component solventborne polyurethane coating which comprises polyacrylic polyol, polyester polyol, and an isocyanate cross-linker and prepared according to technology invented by van Engelen et al.[27] A glass transition temperature of the top coat equals ∼60 °C. Since experiments were performed at 25 °C, the top coat was still in the glassy state, the acrylic core/shell particles of the base coat were at transition between rubbery and glassy state, and PUR particles were at the rubbery state. In the context of this paper, we refer to this sample as the primary BC/TC sample and to its base coat as the primary base coat.

These two-layered films were applied on glass cover slides with an area of 18 × 18 mm^2 and a glass thickness of 150 μm. First, base coats were applied by spraying an aqueous dispersion on the glass slides. After spraying, the base coat was dried at 60 °C for 1 h. The top coat was sprayed on top of the base coat and then cured at 60 °C for ∼20 min. To ensure that the samples were fully cured before using them, the samples were stored for at least 4 weeks at room temperature. Both the base coat and the top coat have thicknesses of ∼50 μm. Gravimetric measurement with a Mettler-Toledo AX205DR analytical balance has shown that water content in the primary sample is low (less than 1.5% w/w).

In order to investigate the role of individual base coat components, a two-layered system with a base coat, containing only the acrylic core/shell particles, and pure PUR films were prepared. The only difference of the two layered system with the primary system is the absence of PUR and pigment particles. Further we refer to this sample as the acrylic BC/TC sample, since it has a pure acrylic base coat. This base coat has a thickness of ∼30 μm. The top coat of this system has a thickness of about 80 μm.

Experimental Setup, Measurements, and Signal Analysis. *Setup.* A NMR setup with a magnetic field B_0 = 1.5 T and a gradient of G = 41 T/m was used. Since a static gradient is used, the effective field of view (FOV) is determined by both the receiver bandwidth and the spectral content of the RF excitation pulse. Pulses with rise and fall times of roughly 0.25 μs and duration of 1 μs were applied, yielding an excitation profile with a width of about 1 MHz (500 μm). The NMR signal was sampled with a frequency of 5 MHz at a receiver bandwidth of 1.5 MHz, resulting in a FOV that is slightly larger than the excitation profile. Home-built NMR equipment was used with acquisition systems described by Kopinga and Pel.[28] Profiles were measured by using an Ostroff−Waugh-like pulse sequence $\theta_x - t_e/2 - [\theta_y - t_e/2 - \text{echo} - t_e/2]_n$ with α nominally equal to 90°.[21,22]

A surface coil with a diameter of 3 mm was used. Samples were put on top of the RF coil. To moisten a sample, a glass tube was glued on top of the coating/film (see Figure 3). A marker at the bottom of the substrate allowed to trace deflections of the substrate and fluctuations of the setup due to instabilities.

Using the one-sided RF coil may lead to the distribution of the RF field. As a result, there will be the distribution of values of θ in the sample. It is assumed that densities of ^{1}H nuclei in the sample are homogeneous in the plane, perpendicular to the x-direction. As a result, the distribution of RF field will not lead to an expression for the signal different than eq 2.

Data Processing. The obtained signals can be described by eq 1. To extract relaxation spectra, the values of $P_n(x)$ have to be

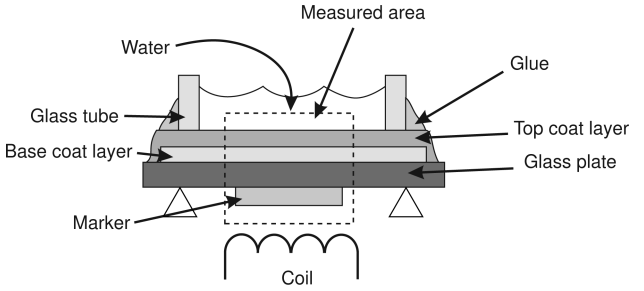

Figure 3. Schematic representation of the experimental setup used for water uptake experiments.

known. To determine the values of $P_n(x)$, a 0.01 m $CuSO_4$ aqueous solution was used as a reference. As the signal of this solution decays monoexponentially, the values of $P_n(x)$ can be determined using eq 2:

$$S_{n,\mathrm{ref}}(x) = \rho_{\mathrm{ref}} P_n(x) \exp\left(-\frac{nt_e}{T_2^{\mathrm{ref}}}\right) \quad (6)$$

where ρ_{ref} [mol/m^3] is the density of ^{1}H nuclei in the $CuSO_4$ solution and $S_{n,\mathrm{ref}}$ [au] is the intensity of the nth echo. The echo trains $S_n(x)$ of the studied samples, described by equation eq 2, can be divided by correction factors obtained from $CuSO_4$ solution data (see eq 6). The corrected signal I_n becomes a simple multiexponential decay and is described in the following equation

$$I_n(x) \equiv \frac{S_n(x)}{S_{n,\mathrm{ref}}(x)\exp(nt_e/T_2^{\mathrm{ref}})} = \sum_k \frac{\rho_k(x)}{\rho_{\mathrm{ref}}} \exp(-nt_e/T_{2k}(x)) \quad (7)$$

Each exponent represents a specific ^{1}H pool with distinct T_2 value. Note that amplitudes of the exponents are relative densities of ^{1}H nuclei with respect to the density of the ^{1}H nuclei in water. Consequently, the factors before each exponent are proportional to concentrations of ^{1}H nuclei.

Considering the main objective of the present study, each of these pools should be identified, their T_2 values should be evaluated and be expressed in terms of ^{1}H quantities n_k. Therefore, measured signal decays were fitted with a regularized inverse Laplace transform algorithm (RILT) as proposed by Venkataramanan et al.,[29] which resulted in T_2 spectra containing a number of peaks. The peaks refer to ^{1}H pools, with a position corresponding to the T_2 values of ^{1}H in the specific pool. The intensities of the peaks reflect the densities ρ_k and the total amount n_k of ^{1}H nuclei if profiles or total signals are treated, respectively. The robustness of the fitting procedure is discussed in Appendix B.

Measurements. In this study we are interested in identifying the contributions of water and polymer to the NMR signal and investigating the state of water in the polymer. For identification of the contributions of water and polymer phases to the signal measurements of the sample in dry, H_2O-wet and D_2O-wet situations were done. They were performed with t_e = 0.1 ms and 8192 averages. The identification experiments were performed with primary and acrylic BC/TC samples and with pure PUR films.

Experiments, dedicated to study the state and mobility of water in the polymer, were performed with t_e ranging from 0.1 to 0.6 ms and with 8192 averages. The primary BC/TC sample was studied in partially and fully saturated states, which were achieved by equilibrating the sample with an aqueous solution of poly(ethylene glycol) (PEG) and liquid water, respectively. The aqueous solution of PEG had a water activity equal to 0.9. This water activity was obtained by tuning the PEG concentration in the solution.[30]

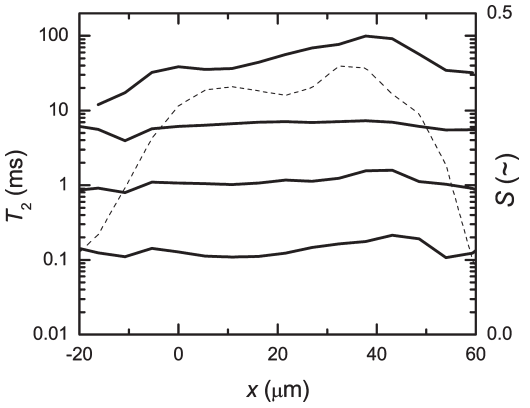

Figure 4. Average T_2 value of each spectral component in the wet base coat of the primary sample as a function of the position. The dashed line represents the signal intensity of the first echo of the coating.

Water uptake in the primary BC/TC sample was measured with t_e = 0.1 ms and 2048 averages. Measurements were performed with a repetition time of t_r = 0.5 ms, resulting in temporal resolution of 20 min. The acquisition time was t_{acq} = 90 μs.

The parameter α in eq 4 was estimated from the signal decay of an 0.01 M aqueous $CuSO_4$ solution. Water in this solution has a $T_2 \simeq 2.6$ ms. The self-diffusion coefficient of water in the $CuSO_4$ solution is equal to 2.5×10^{-9} m^2/s, which is equal to diffusivity of pure water.[31] Using this value and the fact that for $CuSO_4$ solution $T_{2S} \gg T_{2D}$ in our experiments, we obtain that α = 5.

RESULTS

Distinguishing Water and Polymer. *T_2 Relaxation Spectra.* A prerequisite for understanding the interplay of water and the polymer matrix during uptake is that the signals of water and polymeric material can be distinguished. This section focuses on identifying the NMR signal components and assigning them to water and polymeric components (acrylic, PUR, and dispersant).

With the help of the RILT fitting procedure relaxation spectra were obtained for each position in the base coat of the primary BC/TC sample. Four T_2 spectral components were detected at each position in the base coat. The average T_2 values for each component is shown in Figure 4. The dashed line represents the original signal profile $I_n(x)$. The T_2 values are nearly constant as a function of position. Consequently, the properties of each ^{1}H pool, which are reflected by the T_2 value, can be considered as homogeneous in the studied base coat. Concerning the homogeneity, further analysis in our study is based on the total signals of the base coat of the primary BC/TC sample.

The total signal was obtained by integrating the corrected signal in eq 7. As a result, the expression for the total signal I_n^t of the base coat reads

$$I_n^t = \sum_k A_k \exp(-nt_e/T_{2k}) \quad (8)$$

dx.doi.org/10.1021/ma102889u |*Macromolecules* 2011, 44, 4863–4871

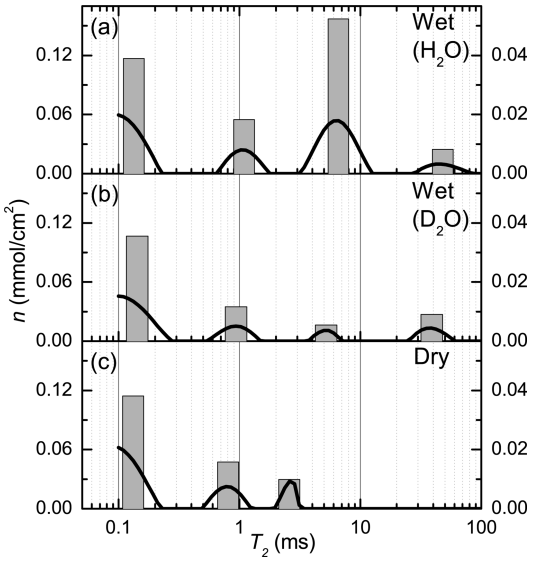

Figure 5. T_2 spectra of the base coat in wet (H_2O (a) and D_2O (b)) and dry (c) states. The bars mark the average spectral positions of the peaks and total intensity of the peaks. The bars intensities are shown by the left scale and the raw spectra intensities are shown by the right scale.

Table 1. Identified Compounds in the Wet Primary Base Coat of the Primary Sample and Their Spectral Positions, for t_e = 0.1 ms

spectral position	0.1 ms	0.8−2.5 ms	6 ms	20−40 ms
compound	acrylic	PUR and dispersant	water	plasticized dispersant

where $A_k \equiv \rho_{ref}^{-1} \int_{BC} \rho_k \, dx$ [μm] reflect a total amount of ^{1}H nuclei in kth pool in the base coat. The density ^{1}H nuclei in liquid water $\rho_{ref} = 0.11$ mol/cm^3. The amount of ^{1}H nuclei n_k [mol/m^2] in kth pool relates to A_k as follows:

$$n_k = \rho_{ref} A_k \quad (9)$$

The solid line in Figure 5a shows the relaxation spectrum obtained from the total signal of the wet base coat. Obviously, there are at least four typical ^{1}H pools that contribute to the signal. The bars show both the average spectral position and the total intensity of the peaks. The total intensity equals the total amount of ^{1}H nuclei in the pool. The next steps in our analysis focus on the identification of the peaks, i.e., understanding the connection of the T_2 components with water and polymeric ingredients of the primary base coat.

Water and Polymer. First, the signal of water in the relaxation spectrum will be identified in Figure 5a. Comparing the spectra of the primary base coat wetted with H_2O (Figure 5a) and wetted with D_2O (Figure 5b) only revealed a significant difference in the intensity of the spectral component at $T_2 \simeq 6$ ms. Whereas in the H_2O-wet spectrum a huge peak exists, this peak is small in the D_2O-wet spectrum. This implies that this spectral component represents water in the base coat (Table 1). The intensity of the water component corresponds to 1.41 mg/cm^2. This value means that the base coat has absorbed ~26% w/w of water. Note that the number of exchangeable protons in hydroxyl, acid, and amine groups in the base coat are equivalent to 0.4% w/w of water in the base coat. Therefore, their amount can be neglected when relaxation spectra are discussed.

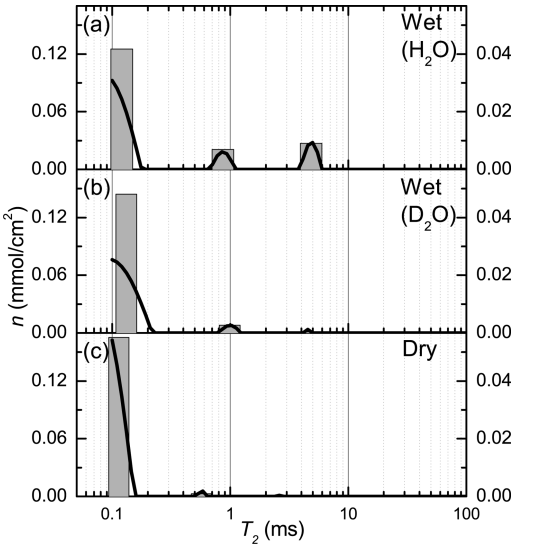

Figure 6. T_2 spectra of the acrylic core/shell base coat in the wet (H_2O (a) and D_2O (b)) and in the dry (c) states. The bars show the average spectral position and the total intensity of the peaks.

As a consequence, all other spectral components are from the polymeric matrix of the coating, which may be sensitive to interaction with water. To detect the influence of water on the polymer matrix, the T_2 spectra of a dry base coat and one wetted with D_2O have to be compared. The spectrum of the dry base coat contains three peaks (see Figure 5). The first component is at $T_2 \simeq 0.1$ ms and two other components are located at $T_2 \simeq 0.9$ ms and $T_2 \simeq 2$ ms, respectively. The spectra of the wet (H_2O and D_2O) system contain a component at $T_2 \simeq 20-40$ ms, which is absent in the spectrum of the dry base coat. Since the T_2 increases drastically due to an increase in polymer mobility, the component at 20−40 ms is a consequence of polymer plasticized by water.

The next step in our analysis is the identification of the acrylic, PUR, and dispersant ingredients among the spectral components of the polymer.

Polymeric Compounds. The pigment particles of the base coat are in a crystalline state and hydrophobic. As they have a T_2 value much less than the used inter-echo time t_e, pigment is not visible in relaxation spectra. Polymeric components in the relaxation spectra in Figure 5 should originate from acrylic core/shell particles, PUR material, and the polymeric dispersant.

In order to identify the T_2 components of the polymer matrix and to determine the polymer compounds that are plasticized by water, the spectra of a base coat of a pure acrylic BC/TC system and of a PUR film are compared with the spectra of the base coat of the primary sample.

The spectra of the base coat of the acrylic BC/TC sample are presented in Figure 6. The spectrum of the dry acrylic base coat contains a single component at ~0.1 ms (see Figure 6c). This implies that the components observed at 0.9 and 2 ms in the spectrum of the dry primary base coat (Figure 5) belong PUR particles and the dispersant. The spectrum of the acrylic base coat wetted with D_2O is presented in Figure 6b. As compared to Figure 6a, it includes a single additional component at 1 ms with negligible intensity; it is concluded that the acrylic core/shell particles are not plasticized by water. We conclude that the shell of the acrylic particles is not distinguished either due to small intensity or due to overlap with the main component at 0.1 ms.

dx.doi.org/10.1021/ma102889u |*Macromolecules* 2011, 44, 4863–4871

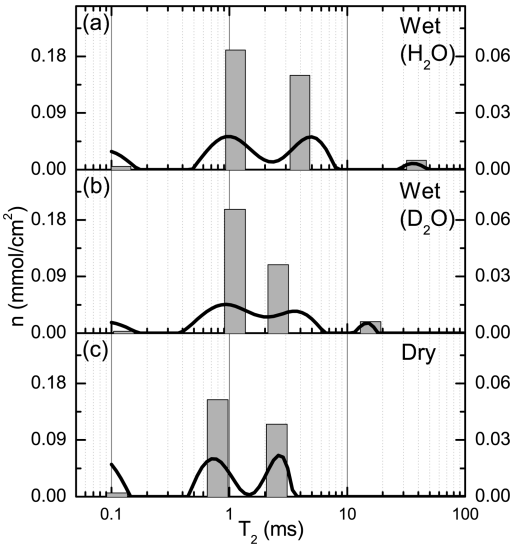

Figure 7. T_2 spectra of the PUR material in the wet (H_2O (a) and D_2O (b)) and in the dry (c) states. The bars show the average spectral position and the total intensity of the peaks.

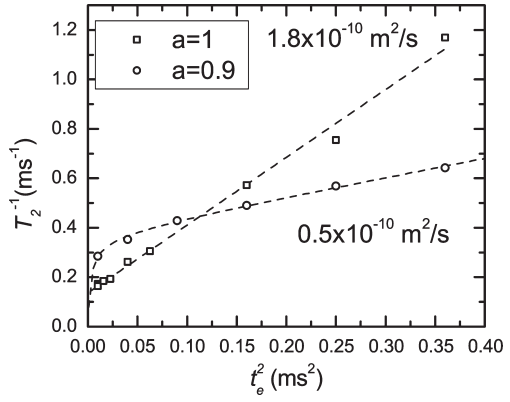

Figure 8. Relaxivity of water in the base primary coat as a function of t_e^2. The base coat was fully saturated (squares) and partially saturated (at a water activity 0.9) (circles). The dashed lines represent linear fit and fit with eq 3 for fully and partially saturated systems, respectively.

The spectrum of the wet acrylic base coat includes two additional T_2 components (see Figure 6a). Since the component at 1 ms is very small and since there is no spectral component at 6 ms in the spectra of dry and D_2O wetted sample, these components represent water in the pure acrylic base coat. Note that the amount of absorbed water is significantly lower than the amount of water taken up by the primary base coat. The analysis of the spectra of the acrylic sample implies that the T_2 component at 20−40 ms observed in the wetted primary base coat (Figure 5) represents plasticized PUR or plasticized dispersant. In order to investigate the contributions of PUR and dispersant to the plasticized material, the PUR film was measured. The relaxation spectra of PUR films are presented in Figure 7. The spectrum of the dry PUR (Figure 7c) contains two T_2 components. Their spectral positions are at 0.8 and 2.5 ms, which are similar to the spectral positions of the nonacrylic components in the primary system (Figure 5c). The spectra of the wetted PUR material feature an extra but small component at 15−40 ms. This component belongs to PUR material, plasticized by water. The intensity of the plasticized PUR component is less than 5% of the total PUR intensity and cannot explain the intensity of the slow relaxing component in the primary sample (see Figure 5a,b). In the primary system the intensity of the plasticized material is 32% of the non-acrylic polymeric components. Note that the mass ratio between the polymeric dispersant and PUR particles in the primary sample was ∼1:2. This implies that in the primary system the component at 20−40 ms is mainly due to the dispersant plasticized by water. Water in the wetted PUR material is represented by component located at ∼4 ms. This position is similar to water spectral position in the primary base coat in Figure 5a. The intensity of the water component equals the difference between intensity of this component and corresponding component in the spectrum of PUR saturated with heavy water (Figure 7b). However, it is significantly lower than the intensity of water component in the primary sample.

A summary of the assignments of the T_2 components is given in Table 1. Thus, in the spectrum of the wet primary base coat (see Figure 5a), we assign the spectral component at 0.1 ms to acrylic core/shell material and the components at 0.8−2.5 ms to the PUR material and the dry dispersant. The component at 20−40 ms mainly belongs to the plasticized dispersant with possibly a very small contribution of plasticized PUR. The spectral component at $T_2 \simeq 6$ ms represents mainly water. Note that the T_2 of water has a smaller value than of the plasticized dispersant. Normally, one would expect that the plasticizer has a similar or higher T_2 value than the plasticized material. The reason may be that either diffusion of water in the field gradient dominates the T_2 relaxation of the water or that protons of water are present at least in two different environments with different mobilities. In the latter case, the measured T_2 time may be affected by a rapid exchange between these environments.[32] Whether or not diffusion explains this observation is discussed in the next section.

An important observation is that the intensity of the water components in the spectra of wet acrylic (Figure 6a) and wet PUR (Figure 7a) materials cannot explain the high intensity of water spectral component in the primary system (Figure 5a). Therefore, we conclude that the hydrophilic PEO/PPO hairs of the polymeric dispersant absorb a significant amount of water.

Diffusivity of Water in the Base Coat. Water in the base coat is either strongly bonded to the polymer or highly mobile. The binding of water to the polymer is reflected by the T_{2S} time, whereas diffusion is described by T_{2D} in eq 3. If water molecules are highly mobile and have a high self-diffusion coefficient, then $T_{2D} \ll T_{2S}$ and $T_2 \simeq T_{2D}$. The goal of this section is to find out whether water binding to the polymer lattice or water diffusion dominates the T_2 value.

Therefore, a primary sample, in fully or partially saturated state, was measured with various echo times ranging from 0.1 to 0.6 ms. The relaxivity T_2^{-1} of water as a function of t_e^2 obtained from the total signal of the fully saturated base coat is shown in Figure 8 (squares). The inverse T_2 increases linearly with t_e^2 and has an offset. This offset seems to be the only influence of T_{2S} in this case, and the echo time dependency of the water relaxation is only determined by diffusion in the field gradient. The slope of the curve of the wet system in Figure 8 equals 2.7×10^9 s^{-3}, which leads to a self-diffusion constant of water of $\sim 1.8 \times 10^{-10}$ m^2/s. This is only 1 decade less than the self-diffusion coefficient of water. This agrees with the observation in our previous study that in this particular system water very quickly redistributes in

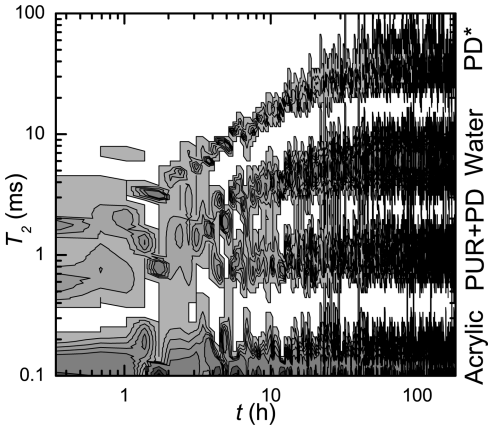

Figure 9. Contour plot of the spectra of the base coat of the primary sample as a function of time during water uptake. The spectra are recorded with t_e = 0.1 ms. PD abbreviation means polymeric dispersant, whereas PD* denotes plasticized polymeric dispersant.

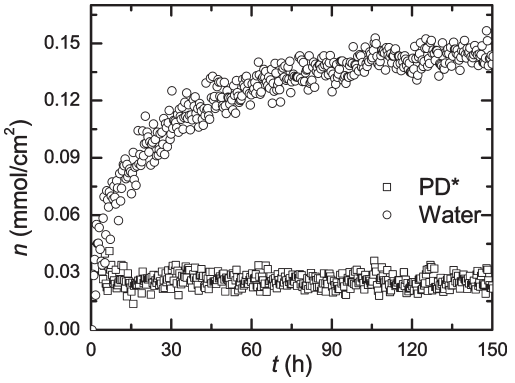

Figure 10. Total intensities of water and plasticized dispersant components as a function of time during water uptake. PD* denotes plasticized polymeric dispersant.

the base coat during water uptake.[12] The value 1.8×10^{-10} m^2/s of the self-diffusion coefficient of water in the fully wet base coat (26% w/w) is similar to values of the diffusivity of water in hydrated hydrogels (20−60% w/w).[33]

The relaxivity T_2^{-1} of water in the partially saturated base coat is shown in Figure 8 (circles). The relaxivity of the partially saturated system has a higher offset value. Further a linear dependency on t_e^2 is only observed for $t_e \geq 0.3$ ms. The slope of the curve in the linear regime equals 0.79×10^9 s^{-3} and is smaller than the one of the fully saturated system. According to eq 4, this value corresponds to a self-diffusion coefficient of 0.5×10^{-10} m^2/s, which is significantly lower than in the completely wet system. That the transition to the linear regime occurs at higher values of t_e than in the case of the completely wet system indicates that the correlation time τ_c for water molecules is longer in the partially saturated system. This is consistent with the increase in the offset.

Therefore, it is concluded that the self-diffusion coefficient of water increases with concentration of water in the polymer and that the binding of water to the polymer is stronger at lower water concentrations. The correlation time of the ^{1}H motions τ_c decreases with the water concentration.

Another conclusion is that the diffusion of water in the field gradient does not explain the previously mentioned observation

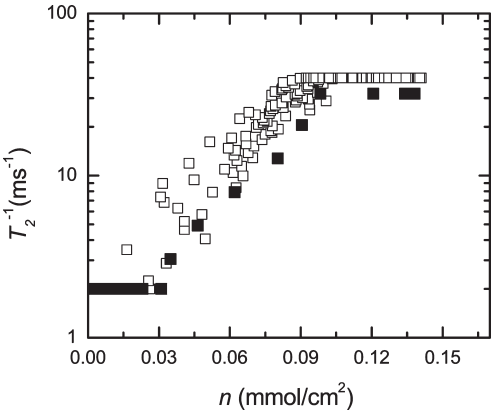

Figure 11. Average relaxation time of the plasticized dispersant in the base coat as a function of the amount of water in the base coat during uptake and drying. An increase of the T_2 indicates an increase of the mobility of the polymeric dispersant.

that T_2 time of water is lower than the T_2 time of the plasticized dispersant. Therefore, the ^{1}H nuclei of water should be present in the base coat at least in two environments, of which one has a low mobility. Further, there has to be a rapid exchange of ^{1}H between these environments. The first environment should be water in the dispersant. The possible candidates for the other environments may be exchangeable protons of the polymeric material (e.g., from hydroxyl, acid and amine groups) or of water molecules which are bounded.

Water and Polymer during Water Uptake. Now the spectra are understood; the evolution of the spectral components during water uptake can be analyzed. Tracking transient behavior of the water spectral component provides information about the amount of absorbed water in the base coat as a function of time. Analyzing the evolution of the spectral component of the dispersant in time gives insight in the process of plasticization during water uptake.

In Figure 9, T_2 spectra of the base coat are plotted as a function of time. The contour plot starts with the spectrum of the dry sample as in Figure 5c and evolves to a four-component spectrum characteristic for a wet sample (Figure 5a). Initially, several components are overlapping in the T_2 range between 0.5 and 2 ms. From Figure 9 we conclude that T_2 values of the acrylic, PUR material, and nonplasticized dispersant do not vary, whereas the T_2 values of water and plasticized dispersant are increasing with time.

The spectral component of water initially appears at $T_2 \sim 1$ ms. During the first 10 h of uptake the T_2 value of water increases until it stabilizes at the spectral position with $T_2 \simeq 6$ ms. The amount of water as a function of time was deduced from the change in total intensity of the spectral components (Figure 10), since water is the only source for new nuclei and the total number of the polymer ^{1}H nuclei is constant during uptake. Fast initial and slow later stages of uptake are observed: half of the water is absorbed during the first 10 h, while an equilibrium is only reached after ∼100 h. The increase of T_2 indicates that the mobility of water also increases in time. Note that these measurements were performed with a t_e = 0.1 ms, and mainly T_{2S} is probed.

The T_2 value of the plasticized dispersant evolves in time from $T_2 \sim 1$ ms to the value of 20−40 ms during ∼30 h. The spectral component of plasticized dispersant cannot be quantified during the first 4 h due to initial overlap of PUR, dispersant, and water

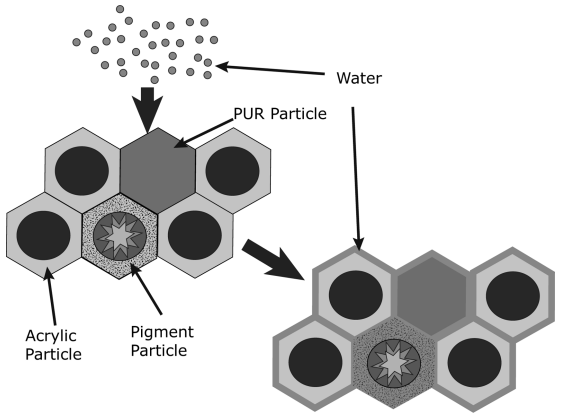

Figure 12. Schematic picture of water uptake. Water is attracted by the hydrophilic elements of the polymer (e.g., hydrophilic shell of acrylic particles and polymeric dispersant) and occupies space between the particles. A large fraction of the water molecules migrate into the dispersant resulting in plasticization of the dispersant material.

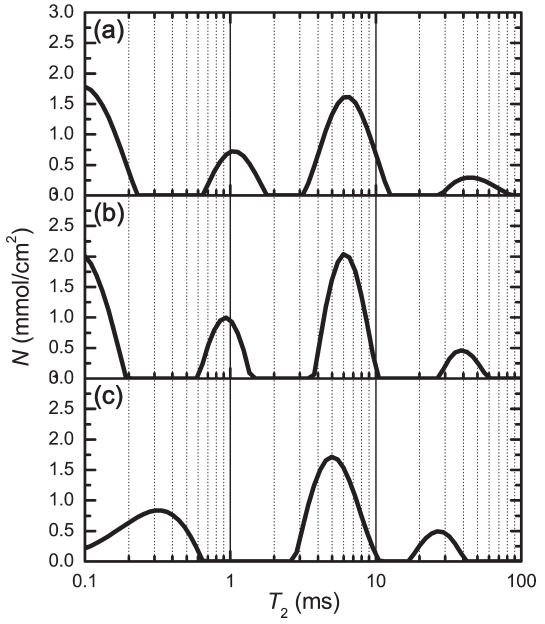

Figure 13. Spectra of a wet base coat of the primary BC/TC sample for the original data measured with 8192 averages (a) and the same data with artificial noise added (the SNR decreased by a factor of 3 (b) and 5 (c)).

spectral components. After 4 h, the total intensity of the plasticized dispersant is constant (see Figure 10). This indicates that all dispersant ^{1}H nuclei susceptible to mobilization are plasticized at low water content.

While the maximal amount of plasticized material has been reached within 4 h, the process of mobilization of these nuclei proceeds up to 30 h. This may be explained by the following: even small amounts of water are enough to mobilize all polymeric chains of the dispersant to a certain degree. With increasing water content the chains obtain more freedom for motions and their T_2 increases with the water content. To check whether or not the T_2 is a unique function of the water content and there is no hysteresis, a drying sample was monitored. The drying process appears to be much faster than uptake ($t \leq 5$ h). The average T_2 values of plasticized dispersant both during uptake and drying were estimated. Figure 11 shows the T_2 of plasticized dispersant as a function of the amount of water both for uptake and drying. Note that there is no significant hysteresis between drying and uptake observed, indicating that there is a unique dependency of the dispersant mobility on the amount of penetrated water.

Combining all results, we suggest Figure 12 for the water uptake process. Water is attracted by hydrophilic areas of the polymer matrix like the shell of the acrylic particles and the polymeric dispersant. A large fraction of the water molecules migrate into the hydrophilic PEO/PPO hairs of the dispersant, causing its plasticization. We suggest that the polymeric dispersant forms a hydrophilic layer near the pigment surface. When water gets into the system, it mobilizes all polymeric chains in this layer. The increase of water content provides more freedom for the polymer chains to move. In addition, the hydrophilic dispersant is an important contributor to the water uptake capacity of the base coat. The relaxation time of water suggests that its protons exchange quickly between at least two environments.

CONCLUSIONS

This study has shown that high-resolution NMR imaging combined with NMR relaxometry is a powerful technique for measuring water uptake in multilayered coatings with multiphase polymer layers. In this particular case, water uptake in a two-layer system was studied that consisted of a highly cross-linked solventborne top coat and a waterborne base coat. The relaxation analysis enabled to identify water and different polymeric compounds in the base coat.

In the considered systems, the self-diffusion coefficient of water in the base coat was estimated. When the base coat was partially saturated the self-diffusion coefficient was 0.5×10^{-10} m^2/s, whereas in the fully saturated state the base coat the self-diffusion coefficient was 1.8×10^{-10} m^2/s. This high value proves that water is highly mobile in the fully saturated base coat, whereas at lower concentrations water is stronger bonded to the polymer matrix of the base coat.

Plasticization of the polymeric dispersant by water was observed, as the mobility of its ^{1}H nuclei increased. A significant number of ^{1}H nuclei in the dispersant became mobilized during water uptake. While this amount was plasticized within 4 h, the mobility of these plasticized domains was still increasing during 30 h. This process appears to be reversible.

It is suggested that initially water is attracted by hydrophilic areas of the polymer matrix, like the shell of the acrylic particles and hydrophilic PEO/PPO hairs of the dispersant. When the water content increases, water becomes mostly located in the hydrophilic part of the dispersant, causing its plasticization and swelling.

APPENDIX A. RELAXOMETRY

In this appendix we discuss the relation between the transversal relaxation time T_2 of diffusing species and the self-diffusion coefficient. The general expression for signal attenuation of protons diffusing in a gradient of the magnetic field was presented by Hurlimann.[18] Because of an inhomogeneous excitation, pathways, contributing to the signal, have unique parameters for each position in the sample. The attenuation of the signal of the

diffusing species reads[18]

$$S(t) \sim \sum_{\{q_k\}} M_{\{q_k\}} \langle \exp(i\phi_{\{q_k\}}) \rangle \tag{10}$$

where $\{q_k\}$ defines a coherent pathway, $M_{\{qk\}}$ is a weighing factor for a coherent pathway and $\phi_{\{qk\}}$ is the phase accumulation during diffusion. In our case subsequent pulses are always separated by intervals t_e. Therefore, the attenuation of a specific coherent pathway due to diffusion reads

$$\langle \exp(i\phi_{\{q_k\}}) \rangle = \exp\left[-\gamma^2 G^2 D t_e{}^2 t \left(\frac{1}{3} \sum_k^N q_k{}^2 + \sum_k^N q_k \sum_l^N q_l (l-1) + \sum_k^N q_k (k-1) \sum_k^N q_l \right) / N \right] \tag{11}$$

where γ [MHz/T] is the gyromagnetic ration, G [T/m] is the gradient of the magnetic field, D [m^2/s] is the self-diffusion coefficient, and $N \equiv t/t_e$ is the number of pulses. Equation 11 can be rewritten as

$$\langle \exp(i\phi_{\{q_k\}}) \rangle = \exp[-\alpha_{\{q_k\}} \gamma^2 G^2 D t_e{}^2 t] \tag{12}$$

It can be concluded that every coherent pathway evolves as a function of a rescaled time $\gamma^2 G^2 D t_e{}^2 t$. Therefore, the overall signal $S(t)$ will always be a function of $\gamma^2 G^2 D t_e{}^2 t$. If the measured signal of diffusing species decays monoexponentially as $\exp(-t/T_{2D})$, the decay time can be described as

$$T_{2D}{}^{-1} = \alpha \gamma^2 G^2 D t_e{}^2 \tag{13}$$

APPENDIX B. BENCHMARKING THE FIT PROCEDURE

To validate the fitting procedure, we have investigated the stability of the RILT fit with respect to the signal-to-noise ratio (SNR) variations.

Artificial noise was added to the original data, which decreases the SNR by factors 3 and 5. The spectra were obtained and compared with the original spectrum of the sample (see Figure 13). A decrease of the SNR by a factor of 3 does not significantly change the number, positions, and amplitudes of the T_2 components. If the SNR is 5 times smaller than in the original data, two components merge to one.

Note that in this study relaxation measurements were performed with 8192 averages and uptake experiments with 2048 (Figure 13a). Therefore, uptake experiments were performed with SNR, which is a factor of 2 lower than SNR in relaxation measurements. Our stability analysis indicates that the SNR during the uptake measurements is suitable for a proper resolution of the T_2 spectra.

AUTHOR INFORMATION

Corresponding Author

*E-mail: h.p.huinink@tue.nl.

ACKNOWLEDGMENT

The project is funded by TU/e, TNO Built Environment and Geosciences, AkzoNobel Automotive & Aerospace Coatings. We thank Hans Dalderop and Jef Noijen from TU/e for technical support and assistance, Klaas Kopinga from TU/e, Taco Scherer and Ruud van Overbeek from AkzoNobel Automotive & Aerospace Coatings for the useful discussions, Kenny Raghosing and Fred Rous from AkzoNobel Automotive & Aerospace Coatings for samples preparation, and Brenda Rossenaar from AkzoNobel RD&I for the TEM study.

REFERENCES

(1) *Paint and Surface Coatings: Theory and Practice*, 2nd ed.; Lambourne, R., Strivens, T., Eds.; Woodhead Publishing Ltd: Cambridge, UK, 1999.
(2) Park, J.; Lee, G.; Ooshige, H.; Nishikata, A.; Tsuru, T. *Corros. Sci.* **2003**, *45*, 1881–1894.
(3) Penon, M. G.; Picken, S.; Wubbenhorst, M.; van Turnhout, J. *J. Appl. Polym. Sci.* **2007**, *105*, 1471–1479.
(4) Allahar, K.; Hinderliter, B.; Tallman, D.; Bierwagen, G. *J. Electrochem. Soc.* **2008**, *155*, F201–F208.
(5) Nguyen, T.; Byrd, E.; Bentz, D.; Lin, C. *Prog. Org. Coat.* **1996**, *27*, 181–193.
(6) Wapner, K.; Grundmeier, G. *Int. J. Adhes. Adhes.* **2004**, *24*, 193–200.
(7) Wapner, K.; Stratmann, M.; Grundmeier, G. *Electrochim. Acta* **2006**, *51*, 3303–3315.
(8) Bosch, P.; Fernandez, A.; Salvador, E. F.; Corrales, T.; Catalina, F.; Peinado, C. *Polymer* **2005**, *46*, 12200–12209.
(9) Wang, W.; Jin, Y.; Su, Z. *J. Phys. Chem. B* **2009**, *113*, 15742–6.
(10) van Der Wel, G.; Adan, O. C. G. *Prog. Org. Coat.* **1999**, *37*, 1–14.
(11) Carbonini, P.; Monetta, T.; Nicodemo, L.; Mastronardi, P.; Scatteia, B.; Belucci, F. *Prog. Org. Coat.* **1996**, *29*, 13–20.
(12) Baukh, V.; Huinink, H. P.; Adan, O. C. G.; Erich, S. J. F.; van der Ven, L. G. J. *Macromolecules* **2010**, *43*, 3882–3889.
(13) Carr, H.; Purcell, E. *Phys. Rev.* **1954**, *94*, 630–638.
(14) Kimmich, R.; Fatkullin, N. *Adv. Polym. Sci.* **2004**, *170*, 1–113.
(15) Adriaensens, P.; Pollaris, A.; Carleer, R.; Vanderzande, D.; Gelan, J.; Litvinov, V. M.; Tijssen, J. *Polymer* **2001**, *42*, 7943–7952.
(16) Glover, P.; Aptaker, P.; Bowler, J.; Ciampi, E.; Mcdonald, P. J. *J. Magn. Reson.* **1999**, *139*, 90–97.
(17) Slichter, C. P. *Principles of Magnetic Resonance*, 3rd ed.; Springer: Berlin, 1990.
(18) Hürlimann, M. D. *J. Magn. Reson.* **2001**, *148*, 367–78.
(19) Sotta, P.; Fülber, C.; Demco, D. E.; Blümich, B.; Spiess, H. W. *Macromolecules* **1996**, *29*, 6222–6230.
(20) Chernov, V. M.; Krasnopolskii, G. S. *J. Exp. Theor. Phys.* **2008**, *107*, 302–312.
(21) Ostroff, E.; Waugh, J. *Phys. Rev. Lett.* **1966**, *16*, 1097–1098.
(22) Mansfield, P.; Ware, D. *Phys. Rev.* **1968**, *168*, 318–334.
(23) Grunder, W.; Schmiedel, H.; Freude, D. *Ann. Phys.* **1972**, *482*, 409–416.
(24) Van Vleck, J. *Phys. Rev.* **1948**, *74*, 1168.
(25) Moos, J.; van Diemen, J.; Broekroelofs, G. Aqueous coating composition comprising an addition polymer and a polyurethane. Patent Application WO 01/48106 A1, July 5, 2001.
(26) Nachtkamp, K.; Mosbach, J.; Noll, K.; Schmitz, H.; Sickert, A. Aqueous coating compositions containing water dispersible polyurethane polyureas as binders and the coatings produced therefrom. US Patent 5141987, Aug 25, 1992.
(27) van Engelen, A.; Koenraadt, M.; van der Putten, A. Coating composition comprising a polyacrylate polyol, a polyester polyol, and an isocyanate-functional crosslinker. Patent Application WO 2007/020269 A1, Feb 22, 2007.
(28) Kopinga, K.; Pel, L. *Rev. Sci. Instrum.* **1994**, *65*, 3673.
(29) Venkataramanan, L.; Song, Y.-Q.; Hürlimann, M. D. *IEEE Trans. Signal Process.* **2002**, *50*, 1017–1026.
(30) Ninni, L. *Thermochim. Acta* **1999**, *328*, 169–176.
(31) Pruppacher, H. *J. Chem. Phys.* **1972**, *56*, 101.
(32) Zimmerman, J.; Brittin, W. *J. Phys. Chem.* **1957**, *61*, 1328–1333.
(33) Ju, H.; Sagle, A. C.; Freeman, B. D.; Mardel, J. I.; Hill, A. J. *J. Membr. Sci.* **2010**, *358*, 131–141.